Ultrasonic Surgical Horn for Approaches to Brain Tumors and Spine Applications

D. J. Cotter, S. Gupta, M. F. Shinopulos, and J. O'Connor
Integra LifeSciences, Burlington MA, USA

***Abstract*— Ultrasonic surgical aspirators are used for removal of tumors in the brain and approaches in spine, where a transducer and horn with a central hole fragment and suction tissue. Bone fragmenting and aspirating surgical tips (horns) are discussed for accessing deeper regions in the brain and for emerging spine applications. Attaining resonant frequency, predicting displacements, and monitoring stress distribution and errant motion are afforded with FEM (Finite Element Method) for emerging complex-contoured horns, complementing one-dimensional physical-mathematical models. A full model method with no artificial constraints and a damped forcing function yields agreement between measured horn displacement and FEM results within 2.5% error (e.g. 5 µm in 224 µm p-p) for the new geometry and baseline horns of this study, and 6.8% error (8 µm in 117 µm p-p) for more complex models.**

Keywords-Ultrasonic Surgical Aspirators, Transducers, Horns

I. Introduction

Ultrasonic surgical aspirators have been used in removal of tumors and tissue in neurosurgery and in gynecological, liver, spine, and orthopedic applications for 30 years [1-5]. As shown in Fig. 1, the transducer is enclosed in a surgical handpiece with a polymer irrigation flue surrounding the titanium horn. A continuous circuit of cooling saline irrigation liquid dilutes blood and further wets aspirated tissue to prevent coagulation and occlusion of the central suction channel of the hollow horn. Small diameter (0.38 mm) preaspiration holes are sometimes used axially near the distal end of the surgical tip to further ensure cooling, prevent occlusion, and capture mist of atomized liquid. The annulus at the distal end of the surgical tip vibrates at ultrasonic frequencies with high amplitudes (e.g., 360 µm p-p). The surgical tip is shown removing a bowel tumor held between the surgeon's thumb and forefinger.

Figure 1. UltrasonicSugical Aspirator. The Tansducer is enclosed in a surgical handpiece with a polymer irrigation flue surrounding the titanium horn. A Tumor is being fragmented and aspirated.

Newly released surgical tips target emergent applications such as the fullest extent of brain surgery through the nose in neuroendoscopy and cutting or abrading bone encountered in approaches [6, 7]. Extending openings in bony cavities or sectioning bone to reveal underlying surgical sites was addressed by developers with specialty ultrasonic devices [8-13]. More recently, spine surgical applications have extended ultrasonic aspiration to foraminotomy, laminar decompression, and bone sculpting.

A. Horn Basis and 1-D Physical Mathematical Models

A modified Kleesattel Gaussian (Ampulla) horn basis is used in surgical tip design and it is published that this geometry affords 60% more amplitude gain for same peak stress as an exponential horn. The horn provides mechanical gain, or more specifically velocity gain, dependent on shape and allowed strain in the material system [14, 15]. A representative cross-sectional area function (1) of a hollow horn with a Gaussian taper outside diameter, straight cylindrical internal diameter, and short straight section at the distal end is solved with area ratio (2) for angular frequency (3). Resonant frequency is dependent on the area ratio and overall length of the surgical tip and can be predicted (4) based on geometry and material properties of the horn.

Horn Gaussian (Ampulla) Profile

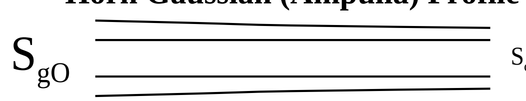

$$S_g(x) = S_{gO} e^{-\frac{1}{2}\left(\frac{\omega_i}{c_g}\right)^2 x^2} \tag{1}$$

$$N = \frac{S_{gO}(\text{Area})}{S_c(\text{Area})} \tag{2}$$

$$\omega_i = \frac{C_g}{L_{tip}}\left(\operatorname{atan}\left(\frac{1}{\sqrt{2\ln(N)}}\right) + \sqrt{2\ln(N)}\right) \tag{3}$$

$$f_i = \frac{\omega_i}{2\pi} \tag{4}$$

After Kleesattel, where ω_i is angular frequency, C_g is the acoustic velocity, L_{tip} is the length of the tip, and f_i is the resonant frequency.

A solid model assembly of a 24 kHz Bone Tip and piezoelectric transducer is shown in Fig. 2. The PZT (Lead Zirconate Titanate) stack transducer, internal stepped horns, and surgical tip are accurately represented in the solid model. Measures (shown with balance symbols) are defined for stack and horn distal end acceleration and displacement. The maximum stress in the surgical tip is monitored. Ultimately, the nodal force is applied uniformly in proximity to the relative node location determined from modal analysis of resonant modes of the model. Surgical horn geometries have become quite complex, as shown in this solid model and picture of a Bone Tip device, with a stepped horn of area ratio gain, Gaussian horn, short straight section, growing exponential, and inverses cone. A helical abrasive pyramidal structure is machined in the inverse cone.

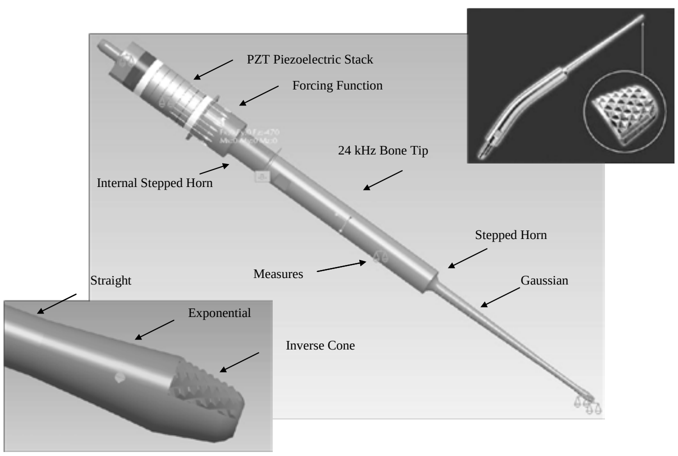

Figure 2. FEM Solid Model. An assembly of a 24 kHz Bone Tip and piezoelectric transducer is shown, along with a picture of the surgical tip. Surgical tip includes a stepped horn, Gaussian, straight section, exponential, and abrasive surface on an inverse cone.

B. *Modeling of Ultrasonic Transducers and Horns*

The 1-D (one-dimensional) physical-mathematical models or equations are still written for the simplified horn geometries, Fig. 3, to provide understanding of parametric adjustment of frequency, gain, and stress; however, complex contours with asymmetric geometries and structure that cannot be practically modeled with physical equations make 3-D FEM (Finite Element Method) essential. The Bone Tip provides examples of the benefit of FEM: as the wall thickness of the horn is increased, frequency increases due to increasing stiffness of a greater wall thickness cylinder, although mass is being added to the horn, and this is not be apparent from the 1-D physical-mathematical model. The pyramidal abrasive structure reduces frequency by about 120 Hz due to the reduction in mass near the antinode, or distal end of the horn. Writing physical equations for this change in geometry and its influence on a resonant frequency dominated by the Gaussian horn is impractical.

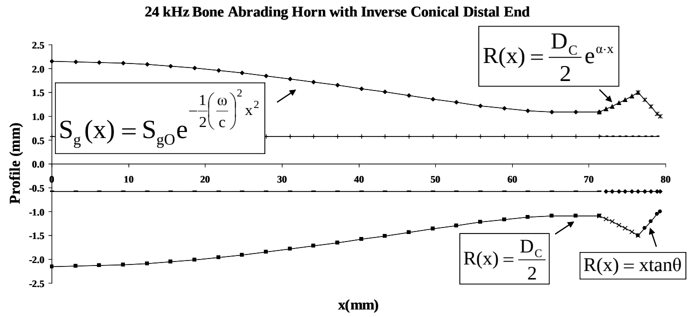

Figure 3. Physical-mathematical Model. Equations are still written for the simplified horn profiles; however, complex contours with asymmetric geometries and structure that cannot be practically modeled with physical equations make 3-D Finite Element Method essential.

Herein, a Pro/Mechanica analysis method published by the authors of this paper is extended from magnetostrictive to piezoelectric transducers, and reference is provided to this earlier publication, which has more discussion of the basic analysis approaches and possible output of results [7]. Pro/Mechanica is a product of Parametric Technology Corporation, Needham MA. Publications provide additional basis for understanding transducer-horn models and mechanics of wave motion [16-20], examples of benefits of FEM [21-22], and indicate another developer used Pro/Mechanica for analyzing ultrasonic horns for welding [23].

II. Approach to Finite Element Method for Surgical Horns, In Brief

Full model approach to Design Frequency Analysis utilizes a forcing function with damping and no artificial constraints. A modal analysis is first executed with the model to determine resonant modes. The force employed in the Design Frequency Analysis (e.g., about 2090 N) is that level provided by transducer stack at 100% amplitude. It is the nodal force and stress at the node that supports strain and elongation necessary to surgical tip stroke. The damping used with the forcing function in Design Frequency Analysis is established to provide the controlled magnitude of stack displacement or known surgical tip displacement. The forcing function analysis of the full model enables the full motion of the components and assembly to be evaluated independent of artificial constraints. Artificial constraints can limit real motion, cause greater frequency resonance due to artificial stiffening of the geometry, and lead to somewhat greater magnitude stress predictions. Artificial surface constraints in a half-model modal analysis can be useful in a wideband analysis (e.g., 5 kHz to 50 kHz) to show the dominant modes associated with the allowed frequencies of the geometry. Full model approach with no artificial constraints yields many modes to be evaluated to determine which are providing predominantly longitudinal motion.

A half model approach with symmetry constraints or full model approach with no artificial constraints will typically be performed over a narrow band about resonance, which may be iteratively reduced to speed processing. The half model approach with symmetry constraints is quite rapid over a narrow band (e.g., 10 minutes of processing time), and it supports iterative design. The half model or sectioned full model also afford unambiguous review of internal stresses of the horn or other components of the assembly.

III. Finite Element Method Output and Simulations

A. Horn Stroke, Stress, and Vibration Simulation

Stroke levels at pertinent locations and relative nodes (local minimum in motion) and antinodes (local maximum in motion) in the horns are shown in Fig. 4. In the present design, the standing wave is orchestrated similarly for the new and baseline horns and the horn stroke is made approximately the same magnitude; consequently, a datum point at the nut of the stack could also be normalized for stroke.

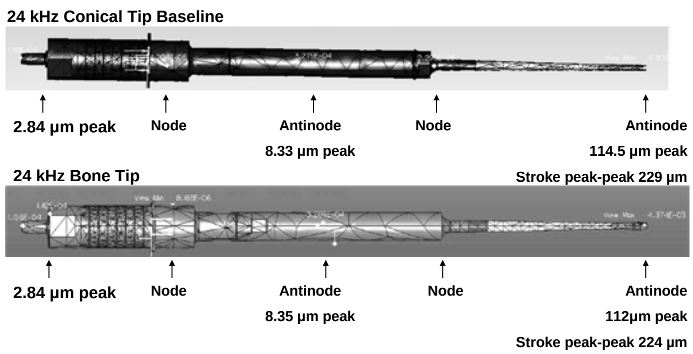

Figure 4. Mechanica Design Frequency Analysis. Stroke levels at pertinent locations and relative nodes and antinodes.

Maximum surgical tip stress locations are exhibited in Fig. 5 for the horn based on a given nodal force in the transducer and achieved stroke. There are many other analysis outputs that are not displayed well in a technical paper; for example, the modal analysis fringe plots show simulated motion dynamically and at selected magnification, so the full motion and any errant modes, such as flexure or ripple are magnified. The Master Interval Analysis enables displacement, stress, strain, velocity, and other selected parameters to be displayed at resonance and queried graphically as a function of position.

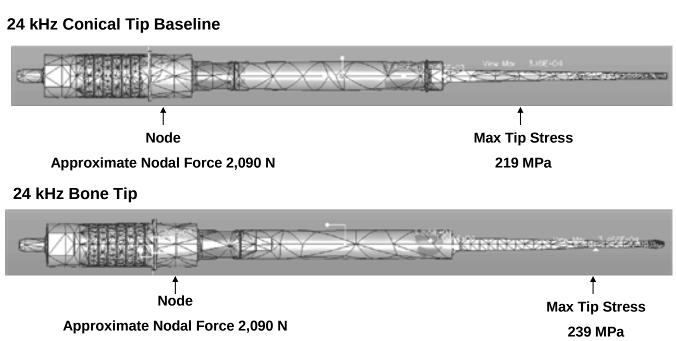

Figure 5. Mechanica Stress Fringe Plots. Maximum surgical tip stress locations are shown for the horn based on a given nodal force.

B. Nodal Force

Mechanica analysis enables calculation of nodal force given known cross-sectional area multiplied by queried stress. It should be noted that damping percentage can be adjusted to establish a known stroke at a datum or distal end of the surgical tip. If the nodal force were initially unknown, a starting value could be entered and the real nodal force determined based on queried stress at a node with the horn at full stroke. Establishing a basis value of nodal force, as well as confirming material properties, with a baseline device is helpful or an iterative approach is necessary. Fig. 6 indicates a potential problem with interrogation of nodal stress or nodal force per unit area at a relative node. High mechanical gain piezoelectric transducers can have large stress concentration due to stepped horns. A query in the stress concentration region could confound determination of nodal force. If a half-wavelength horn extender exists, such that stress is made more planar in the thin-wall, the nodal force could be approximated along the horn. If the relative node is in the radius of curvature of a stepped horn, for example at the end of the extender as shown, the query of nodal stress can be ambiguous due to steep gradients in stress and cross-sectional area.

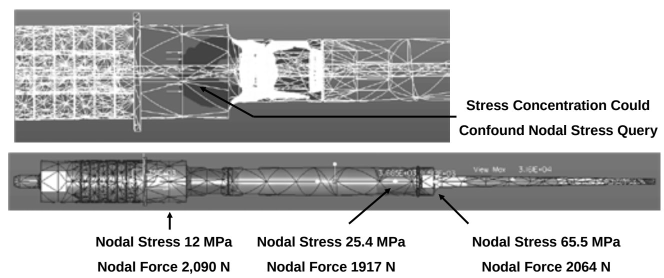

Figure 6. Calculation of Nodal Force. A query in the stress concentration region could confound determination of nodal force. If a half-wavelength horn extender exists, the nodal force could be approximated along the horn. Query of nodal stress can be ambiguous due to steep gradients in stress and cross-sectional area in a radius of curvature.

IV. Summary of Results and Discussion

A. Finite Element Results Tabulated

A summary of Mechanica FEM results is provided in Table 1 for the representative 24 kHz Bone Tip and a 24 kHz Conical Tip baseline device. The results shown are from the Design Frequency Analysis using a full model with a forcing function. Transducer stack peak displacement is normalized at the controlled magnitude about 2.84 µm, which is governed by the closed-loop feedback of the ultrasonic controller. All stress analysis and values displayed herein are based on the von-Misses Stress Criterion. Maximum horn stress yielded by the forcing function analysis of the 24 kHz Bone Tip and 24 kHz Conical Tip baseline device are maintained at approximately 1/3 the yield strength of the titanium. Stress concentrations are also of concern due to potential impact on cyclic fatigue life of the metal. The new horn design results in similar stress to the baseline device. Of course, horns of this design have been successfully employed in surgical applications at similar allowed stress levels for many years. Stroke of the 24 kHz Bone Tip was designed to be about 229 µm p-p, a value similar to the baseline, known to be adequate for precision bone fragmentation. This was favorable to ensuring similar stress levels and operation with the existing analog controller.

Table 1. Summary of Finite Element Analysis

	24 kHz Bone Tip	24 kHz Conical Tip
Stack Displacement peak (µm)	2.84	2.84
Stack Acceleration (m/s^2)	68.6E+3	68.6E+3
Horn von Mises Stress (MPa)	237	219
Horn Stroke peak-peak (µm)	**224**	***229***
Horn Acceleration (m/s^2)	2.69E+06	2.74E+06
Resonant Frequency (Hz)	24,740	24,610
Input Forcing Function (N)	2,091	2,091
Damping (%)	0.01424	0.0848

B. *Experimental Electromechanical Data*

In support of the FEM results, it is important to note that the actual measured strokes of the prototype and baseline horns were in reasonable agreement with Mechanica analysis, as shown in Table 2. Horn stroke is routinely measured optically with a high magnification microscope, CCD camera, monitor, and calibrated “Video Scaler". Data are shown for a sample set of 15 prototype horns and production baseline data. The agreement to the FEM stroke results for the full model and forcing function was within 5 µm for both the new and baseline horns. This represents less than a 2.5% error (e.g. 5 µm in 224 µm p-p) for the new geometry and baseline horn of this study. By incorporating the referenced work by the authors of this paper, 4 other models have shown 2.5 % to 6.8% error (8 µm error in 117 µm p-p) depending on the complexity of the model. Finite Element Method supports horn design, and the analysis coupled with extensive verification and life testing has supported surgical tip development.

Table 2. Electromechanical Data from Fabricated Horns

		Voltage (V_{RMS})	Current (mA_{RMS})	Power (Watts)	Frequency (kHz)	Stroke (µm)
24 kHz Bone Tip	Average	153	288	17	23.87	**229**
	StdDev	21	21	0.6	0.02	3.9
24 kHz Conical Tip	Average	285	477	28	23.76	***229***
	StdDev	11	15	1.0	0.05	3.9

C. *Resonant Frequency Determined*

Modeled resonant frequency of 24,610 Hz for the baseline Conical tip is about 850 Hz greater than the measured electromechanical data of fabricated devices (23,760 Hz), and this frequency shift has been common to all transducer-horn systems analyzed to date. Compliance in the joints is greater than modeled, elastic modulus of titanium material is likely lower than specified, and comparison electromechanical data are acquired at resonance mounted in the handpiece under full stroke quiescent operation, where heating reduces elastic modulus. The new Bone Tip was designed to be closer to an ideal resonance at 24 kHz. Analysis yielded 24, 740 Hz, and given the 850 Hz shift expected, 23,890 Hz was predicted for the new horn. The actual electromechanical data averaged 23,870 Hz, or about a 20 Hz error, and clearly within the range of variance of the material properties and measurements. The Finite Element Method provides a practical means of fabricating tips about resonance in first-pass of machining.

D. *Surgical Bone Tip Employed in Cadaver-Section*

The Bone Tip is shown in Fig. 7 fragmenting and aspirating hard skull bone as the neurosurgeon is comparing removal with other instruments in a cadaver-section. Precision bone removal and thermal management is afforded with the newly released surgical tip.

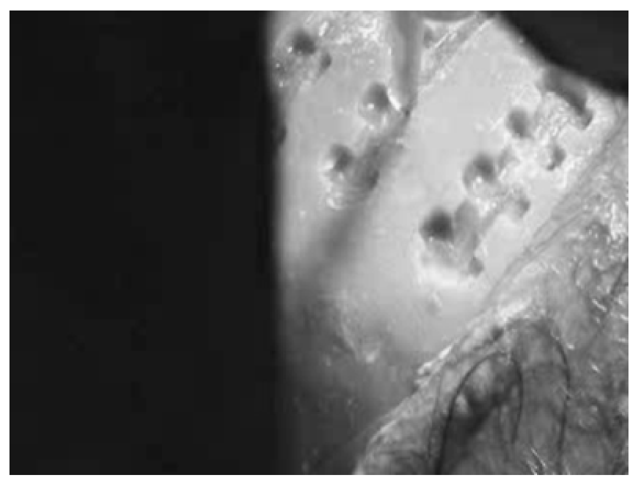

Figure 7. Fragmenting and Aspirating Hard Skull Bone. Precision bone removal and thermal management are afforded with the newly released surgical tip.

V. CONCLUSIONS

Surgical tips with complex contours, asymmetric geometries, and structure that cannot be practically modeled with physical-mathematical equations make 3-D Finite Element Methods essential. Agreement of Finite Element Method results and electromechanical data were within 2.5% error (e.g. 5 µm in 224 µm p-p) for the new geometry and baseline horn of this study. Finite Element Method supports horn design, and analysis afforded coupled with extensive verification and life testing have supported surgical tip development. The Finite Element Method provides a practical means of fabricating tips about design resonant frequency in first-pass of machining. Precision bone removal and thermal management are afforded with the newly released surgical tip.

ACKNOWLEDGMENT

Authors would like to thank Dr. Jeffrey Arle of the Lahey Clinic for aid in testing; Peter Gould, Igor Kosenko, and CUSA Surgical Tip Team for their laboratory, operations, quality, and regulatory efforts; and Peter Colgan, Chris von Jako, and Joe Williams for direction and continued support throughout the course of this work.

REFERENCES

[1] D. G. Wuchinich, A. Broadwin, and R. P. Anderson, “Ultrasonic Aspirator”, U.S. Patent 4 063 557, Dec. 20, 1977.

[2] L. Balamuth, C. Kleesattel, and A. Kuris, “Supply and Control Apparatus for Vibratory Cutting Device”, U.S. Patent 3 213 537, Oct. 26, 1965, Original Application Dec 24, 1954, Ser. No. 477,530.

[3] E. S. Flamm, J. Ransohoff, D. Wuchinich, and D. Broadwin, "A Preliminary Experience with Ultrasonic Aspiration in Neurosurgery”, Neurosurgery 2:240-245;1978.

[4] R. Stoddard and A. J. Reschke, “Ultrasonic Surgical Apparatus”, U.S. Patent 6 124 017, Apr. 10, 2001.

[5] G. Bromfield and J. J. Vaitekunas, “Internal Ultrasonic Tip Amplifier”, U.S. Patent 5 879 364, Mar. 9, 1999.

[6] A. Kassam, C. H. Snyderman, A. Mintz, P. Gardner, and R. L. Carrau, “ Expanded endonasal approach: the rostrocaudal axis. Part I. Crista galli to the sella turcia”, Neurosurg Focus 19(1):E3, 2005.

[7] D.J. Cotter, M. Benson, M.K.M. Smith, J. O’Connor, and M. Shinopulos, “36 kHz Ultrasonic Surgical Horns for Endoscopic-Nasal Approaches to Brain Tumors”, UIA Symposium, March 21, 2007 at the National Physical Laboratory, England.

[8] H. Nakagawa, S. D. Kim, J. Mizuno, Y. Ohara, and K. Ito, “Technical advantages of an ultrasonic bone curette in spinal surgery”, J Neurosurg Spine, 2005 Apr;2(4):431-5.

[9] J. D. Klopfenstein and R. F. Spetzler, “Ultrasonic Aspirator Tip Variations: Instrumentation Assessment”, Barrow Neurological Institute, St. Joseph’s Hospital and Medical Center, Phoenix, Arizona, Barrow Quarterly Vol. 20, No. 3, 2004.

[10] Y. Satou, “Ultrasonic Hand Piece and Ultrasonic Horn For Use With Same”, U.S. Patent 6 497 715 B2, Dec. 24, 2002.

[11] J. C. Easley, E. J. Timm, and R. F. Spetzler, “Torsional Pineapple Dissection Tip”, U.S. Patent Application Pub., US2006/0004396, Jan. 5, 2006.

[12] D. G. Wuchinich, “ Longitudinal-Torsional Ultrasonic Tissue Dissection”, U.S. Patent Application Pub., US2005/0264139, Dec. 1, 2005.

[13] D. G. Wuchinich, “ Longitudinal-Torsional Ultrasonic Tissue Dissection”, U.S. Patent Application Pub., US2001/0047166, Nov. 29, 2001.

[14] C. Kleesattel, Acustica 12[1962], 322.

[15] E. Eisner and J. S. Seager, “A Longitudinally Resonant Stub for Vibrations of Large Amplitude”, SMRE, Research Report No. 216, October, 1963, pp 1-51.

[16] W. P. Mason and R. F. Wick,” J. Acoust. Soc. Am. 23, 209-214 (1951).

[17] P. M. Morse, *Vibration and Sound*, 2nd ed. Published by American Institute of Physics for the Acoustical Society of America, 1976.

[18] G. R. Baldock and T. Bridgeman, *The Mathematical Theory of Wave Motion*, Chichester, West Sussex, England: Ellis Horwood Limited, 1981.

[19] J. Krautkramer J. and H. Krautkramer, *Ultrasonic Testing of Materials*, Berlin, Heidelberg, New York, 1983.

[20] D. Ensminger, *Ultrasonics Fundamentals Technology Applications*, 2nd ed., New York:Marcel Dekker, Inc, 1988.

[21] S. Sherrit, B. P. Dolgin, Y. Bar-Cohen, D. Pal, J. Kroh, and T. Peterson, “Modeling of Horns for Sonic/Ultrasonic Applications”, in *Proc.* IEEE Ultrasonics Symposium, 1999, pp 647-651.

[22] S. Sherrit, S. P. Leary, B. P. Dolgin, and Y. Bar-Cohen, “Comparison of the Mason and KLM Equivalent Circuits for Piezoelectric Resonators in Thickness Mode”, in *Proc.* IEEE Ultrasonics Symposium, 1999.

[23] L. Parrini, “New Methodology for the Design of Advanced Ultrasonic Transducers for Welding Devices”, in *Proc.* IEEE Ultrasonics Symposium, 2000.